

## Observation of an inverse Doppler shift from left-handed dipolar spin waves

Daniel D. Stancil,\* Benjamin E. Henty, Ahmet G. Cepni, and J. P. Van't Hof

*Department of Electrical and Computer Engineering, Carnegie Mellon University, Pittsburgh, Pennsylvania 15213, USA*

(Received 16 March 2006; revised manuscript received 3 August 2006; published 30 August 2006)

We report the experimental observation of an inverse Doppler shift from the motion of an ordinary solid object. The experiment used left-handed, or backward, spin waves in a magnetic thin film. As a pick-up antenna was moved toward the spin wave source, the measured frequency decreased. In contrast, an increase would be expected in everyday experience as the observer approaches the source. The backward spin wave wavelength in the experiment was 1.83 mm at 3 GHz, resulting in a Doppler shift of 546 Hz sec/m, or about 50 times larger than would be observed on an ordinary electromagnetic wave at the same frequency. The measured shifts and dispersion relation agree well with the established theory.

DOI: [10.1103/PhysRevB.74.060404](https://doi.org/10.1103/PhysRevB.74.060404)

PACS number(s): 75.30.Ds, 78.20.Ls, 41.20.Jb, 85.70.Kh

The Doppler shift<sup>1</sup> is familiar in common experience as the change in pitch when we are moving relative to a sound source such as a siren. When we move toward the source, the pitch sounds higher. This phenomenon occurs for electromagnetic waves as well as sound waves, and is used in applications such as radar and motion detection. The possibility of an inverse or anomalous Doppler shift has been recognized in certain physical systems.<sup>2-7</sup> In a system with an inverse Doppler shift, the pitch would sound lower when the observer moves toward the source. To date the only observation of an inverse shift involved waves reflecting from a nonlinearity caused by a pump pulse in a nonlinear transmission line.<sup>3</sup> Here we report the observation of an inverse Doppler shift resulting when the electromagnetic fields from left-handed dipolar spin waves are detected using an antenna on a solid moving object. Neither the inverse Doppler shift resulting from the motion of solid objects, nor the inverse shift from left-handed waves has previously been observed. We found that the spin wave wavelengths determined experimentally from the Doppler shift agreed well with measurements obtained from the frequency dependence of the phase retardation in the absence of motion. These measurements were also found to be in good agreement with the theory of spin wave propagation in a thin film above a ground plane. Our results provide a demonstration using ordinary solid objects of a basic physical phenomenon that has been discussed in the literature for more than 40 years, and may suggest a method for verifying the backward wave nature of artificial metamaterials engineered to be left-handed.

To understand the origin of the inverse Doppler effect, we note that the shift in frequency is determined by the relative directions of the phase velocity of the wave and the direction of motion, and in the nonrelativistic limit is given by<sup>1</sup>

$$\Delta f = -\frac{v}{\lambda} \cos \theta, \quad (1)$$

where  $v$  is the velocity magnitude (speed) of the observer,  $\lambda$  is the wavelength, and  $\theta$  is the angle between the velocity of the observer and the phase velocity of the wave. Consequently, if the direction of either the observer velocity or the phase velocity of the wave reverses, the Doppler shift will change sign.

As pointed out by Veselago,<sup>5</sup> an inverse Doppler shift

should occur in media for which the electric field intensity  $\mathbf{E}$ , the magnetic field intensity  $\mathbf{H}$ , and the direction of the movement of the constant phase planes (described by the wave vector  $\mathbf{k}$ ) form a left-handed coordinate system—in contrast to the right-handed system formed by these vectors in an ordinary medium. As a result, the phase velocity and energy velocity would be oppositely directed, giving rise to what is called a backward wave. Veselago specifically considered a material in which the permittivity and permeability were simultaneously negative. Although such a material did not then exist, Veselago showed that such a material would have a number of other interesting properties, including an inverse Cerenkov effect and negative refraction as well as an inverse Doppler effect. Interest in Veselago's observations has grown following the recent proposal and realization of artificial materials with simultaneous negative permittivity and permeability.<sup>8-11</sup> However, we emphasize that the inverse Doppler shift should occur in any system that exhibits backward wave behavior; materials with simultaneous negative permittivity and permeability are but one example.

In our experiment, the inverse Doppler shift is realized using backward dipolar spin waves in a magnetic thin film. A receiving probe on a rotating element periodically moves across the surface of the film, creating relative motion between the source and observer. The short wavelengths of the spin waves enhance the magnitude of the Doppler shift by factors of 50–70 over what would be expected from electromagnetic waves in free space. Large inverse Doppler shifts should also be observed using other slow backward wave excitations such as left-handed surface polaritons,<sup>12</sup> magnetoinductive waves,<sup>13</sup> and electroinductive waves.<sup>14</sup> Other backward wave systems have been demonstrated,<sup>15-17</sup> though smaller Doppler shifts will be exhibited as the wavelength becomes comparable to that of free space.

It is well known that backward dipolar spin waves propagate in a magnetic thin film with saturated in-plane magnetization when the direction of propagation is parallel or antiparallel to the applied magnetic field.<sup>18,19</sup> This behavior results from the anisotropic nature of the propagation of spin waves in a saturated ferromagnet or ferrimagnet coupled with the boundary conditions at the surfaces of the film. The range of frequencies over which these spin waves propagate is referred to as the spin wave manifold.

The properties of these spin waves are dominated by the magnetic energy densities associated with the waves, and are

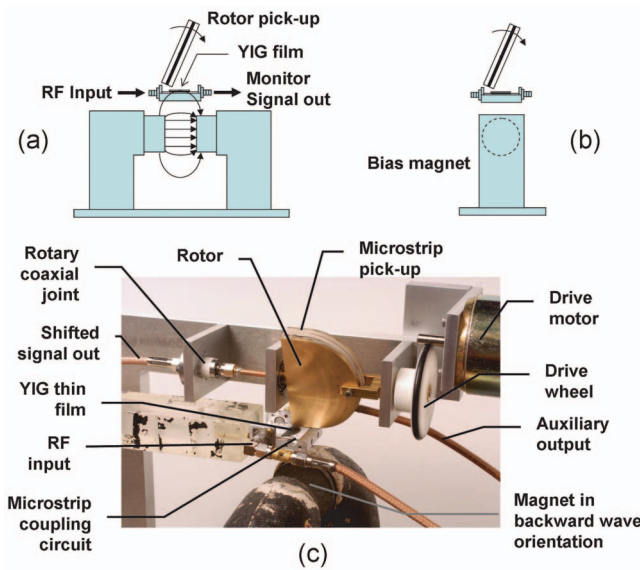


FIG. 1. (Color) Experimental configuration for the Doppler shift measurements. Spin waves are excited in the magnetic thin film and sensed by a moving microstrip antenna on a rotating pickup. (a) Diagram of test geometry with bias magnet in the orientation for left-handed (backward) waves. (b) Diagram with bias magnet in the orientation for right-handed (forward) waves. (c) Photograph of test setup. The Doppler-shifted rf output from the rotor passes through a rotary coaxial joint to the upper left (magnet shown in the orientation for left-handed waves).

well described by models based on the magnetoquasistatic form of Maxwell's equations. In these models, the electric field is ignored and the dielectric properties of the medium have no impact on the properties of the waves (note also that the permittivity is positive). However, a first-order electric field can be derived using the quasistatic magnetic fields, and the flow of energy associated with the wave is given accurately by the electromagnetic Poynting vector  $\mathbf{S} = \frac{1}{2} \text{Re}\{\mathbf{e} \times \mathbf{h}^*\}$ , where  $\mathbf{e}$  and  $\mathbf{h}$  are the small-signal components of the electric and magnetic field intensities, respectively.

Consider a geometry in which a magnetic film is placed in the  $x$ - $z$  plane between two semi-infinite dielectric regions, with an in-plane static magnetic bias field applied along the  $\hat{z}$  direction. We are interested in waves that are guided along the  $\hat{z}$  direction by reflecting from the top and bottom surfaces of the film. In the magnetoquasistatic model, the small-signal magnetic field intensity can be expressed as  $\mathbf{h} = -\nabla\psi(y, z)$ , where  $\psi$  is a scalar potential function. Here no  $x$  variations exist since the propagation is entirely in the  $y$ - $z$  plane. It follows that there is no  $x$  component of the magnetic field intensity, so the field components contributing to the flow of energy along the  $z$  direction are  $e_x, h_y$ . The potential function  $\psi$  for the lowest-order backward wave mode in this geometry is given in Ref. 19. Using this potential function and assuming propagation with positive wave number  $\beta$  where  $\psi \sim \exp(i\beta z - i\omega t)$ , the  $y$  component of the magnetic field intensity can be readily found. An estimate of the first-order electric field  $e_x$  can then be obtained using Maxwell's equation from Faraday's law along with the constitutive relation

$b_y = \mu_{22} h_y$ , where  $\mu_{22} = \mu_0$  in the dielectric regions and  $\mu_{22}$  in the film is obtained from the general permeability tensor for a lossless microwave magnetic material saturated along the  $z$  direction, and is given by<sup>20</sup>

$$\mu_{22} = \mu_0 \frac{\omega_0(\omega_0 + \omega_M) - \omega^2}{\omega_0^2 - \omega^2}. \quad (2)$$

Here  $\omega_0 = -\gamma\mu_0 H_{DC}$ ,  $\omega_M = -\gamma\mu_0 M_S$ ,  $H_{DC}$  is the magnitude of the static magnetic bias field,  $M_S$  is the saturation magnetization of the film,  $\mu_0$  is the permeability of free space, and  $\gamma/(2\pi) = -28$  GHz/T is the gyromagnetic ratio. The frequencies at which the numerator and denominator vanish correspond to the upper and lower edges, respectively, of the spin wave manifold. Consequently  $\mu_{22} < 0$  in the magnetic film over the entire spin wave manifold. Both  $e_x$  and  $h_y$  have a cosine behavior through the thickness of the film and decay exponentially in the dielectric regions.

The direction of the phase velocity is the same as the direction of the in-plane wave vector defined by  $\boldsymbol{\beta} = \hat{z}\beta$ . To establish whether or not the wave is left-handed, we therefore examine the sign of the quantity  $\boldsymbol{\beta} \cdot (\mathbf{e} \times \mathbf{h}^*)$ , since if this quantity is negative, the transverse components of  $\mathbf{e}$  and  $\mathbf{h}$  necessarily form a left-handed triplet with  $\boldsymbol{\beta}$ . Using the aforementioned expressions for  $e_x$  and  $h_y$ , we find that  $\boldsymbol{\beta} \cdot (\mathbf{e} \times \mathbf{h}^*)$  is negative inside the film indicating left-handed fields, but positive outside the film indicating right-handed fields. When  $\boldsymbol{\beta} \cdot (\mathbf{e} \times \mathbf{h}^*)$  is integrated over a cross section unbounded in the  $\pm y$  directions, the energy flow inside the film dominates, and the guided mode has a net left-handed behavior, i.e.,  $\int_{-\infty}^{\infty} \boldsymbol{\beta} \cdot (\mathbf{e} \times \mathbf{h}^*) dy < 0$ .<sup>21,22</sup>

Having established the left-handed (and thus backward wave) character of the guided spin wave modes of the magnetic film magnetized in-plane, it follows that the waves should exhibit an inverted Doppler shift as argued by Veselago. The magnitude of the Doppler shift from spin waves can be orders of magnitude larger than that from electromagnetic waves in free space at the same frequency, owing to the short wavelengths of the spin waves.

The apparatus used in the experiments is shown in Fig. 1. A ferrimagnetic thin film of yttrium iron garnet (YIG) epitaxially grown on a substrate of gadolinium gallium garnet (GGG) is used to support the left-handed spin waves. The film is  $65 \mu\text{m}$  thick and is present on only one side of a  $530 \mu\text{m}$  GGG substrate. The spin waves are excited by placing the magnetic sample film-side-down on a  $50 \mu\text{m}$  wide microstrip antenna fabricated on a  $254 \mu\text{m}$  thick alumina substrate. The alumina substrate is coated with a metallic ground plane on the opposite side, and is attached to an aluminum holder using silver epoxy. (The presence of the ground plane introduces an asymmetry that perturbs the fields for small  $\beta$ , but does not impact the backward nature of the mode.) Above the film and within  $180 \mu\text{m}$  of the surface is located a rotor with a similar microstrip pickup antenna, but fabricated on a flexible microstrip substrate to allow conformance to the shape of the rotor. The signal from this rotating pick-up antenna is coupled back to the measuring instrumentation using a rotary coaxial joint. The rotation sense and speed of the rotor are determined by a dc motor

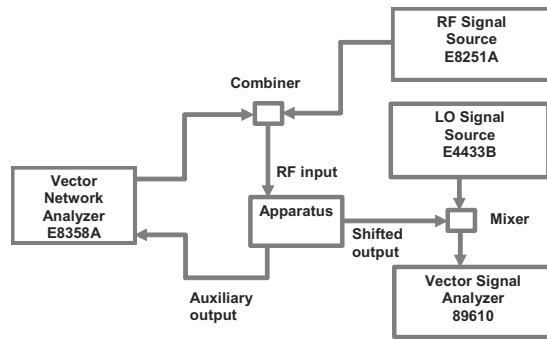


FIG. 2. Measurement system configuration. Excitation was provided by the network analyzer for delay line transmission response measurements, while the rf signal generator was used for the Doppler measurements. Only one source was operating at a time.

coupled via a drive pulley. An auxiliary output is also available on the stationary microstrip circuit to permit characterization of the spin waves excited in the film independent of the rotating pickup. Because the coupling to the spin waves occurs only during a small portion of the rotation cycle when the pickup is closest, to a good approximation the tangential velocity is parallel ( $\theta=0$ ) or antiparallel ( $\theta=\pi$ ) to the wave vector when the signal is detected. Thus the Doppler shift is  $\Delta f = \mp v/\lambda$ , where  $v$  is the tangential velocity of the rotating pickup antenna. The sense of rotation was such that the pickup was always moving toward the source of the spin waves.

The in-plane magnetic bias field is supplied by the permanent magnet shown below the fixture containing the magnetic thin film. The magnet can be rotated about a vertical axis so that the field can be either parallel or transverse to the direction of propagation. When the field is transverse, forward surface spin waves are excited for comparison with the backward waves.<sup>18,19</sup> The Doppler shift from these forward surface waves has been previously reported.<sup>23</sup>

The measurement system is shown in Fig. 2. An Agilent E8358E network analyzer and an Agilent E8251A RF signal source were used one at a time to provide excitations to the apparatus. The network analyzer connected to the auxiliary output was used to measure the spin wave transmission response, while the rf signal source was used to provide the cw input used with the Doppler shift measurements. The Doppler shifted signal output was downconverted to 20 MHz using a mixer and an Agilent E4433B signal generator used as a local oscillator. The spectrum of the 20 MHz signal was obtained using an Agilent 89610 vector signal analyzer in the spectrum analyzer mode. The frequency resolution of the spectral measurements was 4 Hz.

The signal from the left-handed spin waves with the rotor stationary is shown in Fig. 3(a). It simply shows a clean, narrow-band signal from the rf source. When the rotor is in motion, a series of rf pulses is received [Fig. 3(b)] from which both the rotation rate and the Doppler shift can be obtained. Since the pickup was moving toward the source of the spin waves, an increase in frequency would normally be expected. However, a negative Doppler peak from the left-handed waves is clearly evident in Fig. 3(c). For comparison, the spectrum for the right-handed surface waves is shown in

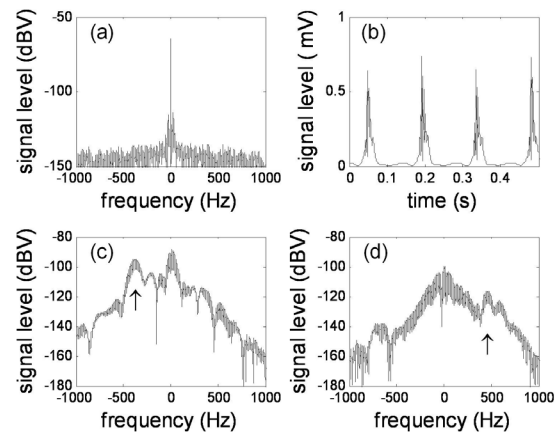


FIG. 3. Frequency spectra and time envelopes of measured signals. (a) Signal spectrum with no rotation showing a clean single frequency excitation. (b) Signal pulse envelopes from left-handed (backward) waves with a rotation rate of 208.2 rpm. Signal pulses are created twice during each pickup rotation as the antennas pass near the film. (c) Signal spectrum centered at 3.01 GHz from left-handed waves with a rotation rate of 208.2 rpm. A downshifted peak showing the inverted Doppler shift is apparent. (d) Signal spectrum centered at 3.61 GHz from right-handed (forward) waves with a rotation rate of 208.6 rpm. In this case, an up-shifted peak is observed as expected from everyday experience.

Fig. 3(d). In this case, a positive Doppler peak can be clearly seen. The fine structures shown in Figs. 3(c) and 3(d) are the harmonics of the pulse repetition period which are just resolved by the 4 Hz resolution bandwidth of the spectrum measurements. We would like to emphasize that the input connector and direction of rotation were not changed between Figs. 3(c) and 3(d); the only difference is rotating the bias magnet by  $90^\circ$  and changing the frequency to correspond to the appropriate wave.

The Doppler shifts as a function of rotation rate for both the left-handed (backward volume) and right-handed (forward surface) waves are shown in Fig. 4. From these measurements and Eq. (1), the backward and forward spin-wave wavelengths were determined to be 1.83 and 1.46 mm, respectively. These are to be compared with the free space electromagnetic wavelength at 3 GHz of 100 mm. The points on the dispersion diagram corresponding to these values are shown by the circles in Fig. 5. Also shown in Fig. 5 are the theoretical dispersion relations for backward volume spin waves and forward surface spin waves including the effects of the microstrip ground plane.<sup>19,24</sup> A Hall probe was used to measure the magnetic field strength at the approximate location of the film. However, since the film was located in a region of nonuniform fringing fields from the magnet, the field was also used as an adjustable parameter in the theoretical fit. The value of 43 kA/m (540 Oe) obtained from the fit agreed well with the Hall measurement. Finally, Fig. 5 also shows the dispersion relations derived from analyzing the auxiliary output with a vector network analyzer. The phase measured from the auxiliary output relative to the input is  $\beta L$  modulo  $2\pi$ , where  $L$  is the propagation distance between the input and auxiliary antennas. Consequently the dispersion relation can be obtained by adding multiples of



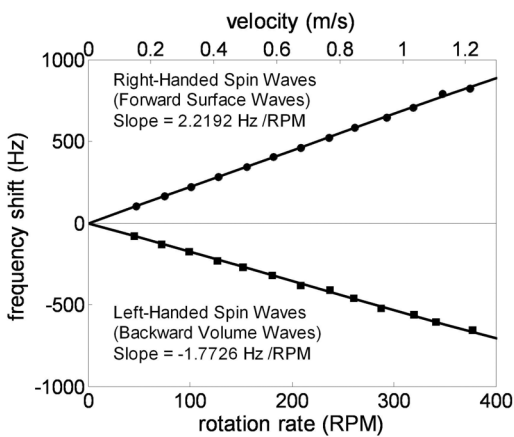


FIG. 4. Doppler shifts obtained as the rotation rate is varied. The tangential linear velocity is given across the top axis. The left-handed waves generate a negative shift, while the right-handed waves generate a positive shift.

$2\pi$  to “unwrap” the phase. After adding appropriate multiples of  $2\pi$  to make the curve continuous, an overall offset of a multiple of  $2\pi$  is added to obtain the best agreement with the theory. Note that although shown on the same diagram, the backward wave and forward wave data were obtained in separate measurements with the bias magnet rotated by  $90^\circ$  between measurements. Also note that the backward wave dispersion relation is shown on the left side of the vertical axis so that the sign of  $\beta$  changes but the sign of the group velocity (slope of the dispersion relation) remains positive. This reflects the fact that the energy must always propagate away from the source, so it is the phase velocity rather than the group velocity that changes sign for the backward wave.

In summary, the inverse Doppler shift arising from left-handed dipolar spin waves has been experimentally ob-

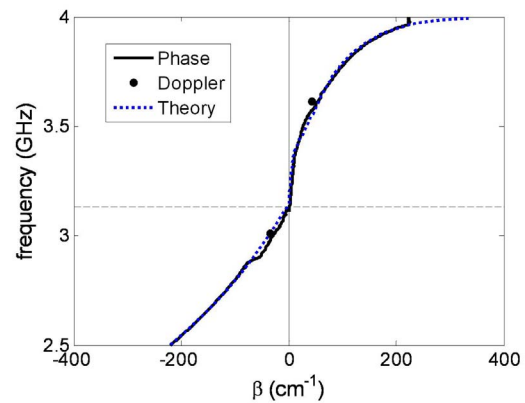


FIG. 5. (Color online) Spin wave dispersion relations. The curve labeled “Phase” was obtained by unwrapping the phase measured from the auxiliary signal output, the points labeled “Doppler” were obtained from the slopes in Fig. 4, and the theory is the conventional theory for spin waves in a thin film above a ground plane (Ref. 24).

served. The shift is caused by the motion of a solid moving object on which a pickup antenna is mounted. The observed shifts are 50–70 times larger than would be observed with free electromagnetic waves at the same frequency, owing to the short wavelength of the spin waves. Points on the dispersion relation inferred from the Doppler measurements agree with the dispersion relation obtained from analyzing the spin wave phase from the auxiliary output, and both of these experimental measurements are in good agreement with theoretical calculations of the dispersion relations.

The thin film of yttrium iron garnet used in these experiments was provided by Devlin Gaultieri. This material is based in part upon work supported by the National Science Foundation.

\*Electronic address: stancil@cmu.edu

- <sup>1</sup>J. D. Jackson, *Classical Electrodynamics*, 2nd ed. (Wiley, New York, 1975), p. 509.
- <sup>2</sup>M. Einat and E. Jerby, *Phys. Rev. E* **56**, 5996 (1997).
- <sup>3</sup>N. Seddon and T. Bearpark, *Science* **302**, 1537 (2003).
- <sup>4</sup>I. M. Frank, *J. Phys. (USSR)* **7**, 49 (1943).
- <sup>5</sup>V. G. Veselago, *Usp. Fiz. Nauk* **92**, 517 (1968) [*Sov. Phys. Usp.* **10**, 509 (1968)].
- <sup>6</sup>N. Engheta, A. R. Mikelson, and C. H. Papas, *IEEE Trans. Antennas Propag.* **AP-28**, 519 (1980).
- <sup>7</sup>E. J. Reed, M. Soljacic, and J. D. Joannopoulos, *Phys. Rev. Lett.* **91**, 133901 (2003).
- <sup>8</sup>J. B. Pendry, A. J. Holden, W. J. Stewart, and I. Youngs, *Phys. Rev. Lett.* **76**, 4773 (1996).
- <sup>9</sup>J. B. Pendry, A. J. Holden, D. J. Robbins, and W. J. Stewart, *IEEE Trans. Microwave Theory Tech.* **47**, 2075 (1999).
- <sup>10</sup>D. R. Smith, W. J. Padilla, D. C. Vier, S. C. Nemat-Nasser, and S. Schultz, *Phys. Rev. Lett.* **84**, 4184 (2000).
- <sup>11</sup>R. A. Shelby, D. R. Smith, and S. Schultz, *Science* **292**, 77 (2001).
- <sup>12</sup>R. Ruppin, *J. Phys.: Condens. Matter* **13**, 1811 (2001).

- <sup>13</sup>E. Shamonina, V. A. Kalinin, K. H. Ringhofer, and L. Solymar, *J. Appl. Phys.* **92**, 6252 (2002).
- <sup>14</sup>M. Beruete, F. Falcone, M. J. Freire, R. Marqués, and J. D. Baena, *Appl. Phys. Lett.* **88**, 083503 (2006).
- <sup>15</sup>P. E. Mayes, *Proc. IRE* **49**, 962 (1961).
- <sup>16</sup>G. V. Eleftheriades, A. K. Iyer, and P. C. Kremer, *IEEE Trans. Microwave Theory Tech.* **50**, 2702 (2002).
- <sup>17</sup>J. A. Kong, *Electromagnetic Wave Theory* (EMW Publishing, Cambridge, MA, 2005), p. 221.
- <sup>18</sup>R. W. Damon and J. R. Eshbach, *J. Phys. Chem. Solids* **19**, 308 (1961).
- <sup>19</sup>D. D. Stancil, *Theory of Magnetostatic Waves* (Springer-Verlag, New York, 1993), pp. 107–117.
- <sup>20</sup>D. M. Pozar, *Microwave Engineering*, 2nd ed. (Wiley, New York, 1998), p. 503.
- <sup>21</sup>S. S. Gupta and N. C. Srivastava, *IEEE Trans. Microwave Theory Tech.* **MTT-28**, 915 (1980).
- <sup>22</sup>S. S. Gupta, *IEEE Trans. Magn.* **MAG-18**, 1639 (1982).
- <sup>23</sup>N. L. Koros, D. D. Stancil, and N. Bilaniuk, *J. Appl. Phys.* **67**, 511 (1990).
- <sup>24</sup>N. D. J. Miller, *Phys. Status Solidi A* **43**, 593 (1977).